

# Different Phenotypes Represent Advancing Stages of *ABCA4*-Associated Retinopathy: A Longitudinal Study of 212 Chinese Families From a Tertiary Center

Yingwei Wang, Wenmin Sun, Jing Zhou, Xueqing Li, Yi Jiang, Shiqiang Li, Xiaoyun Jia, Xueshan Xiao, Jiamin Ouyang, Yueye Wang, Lin Zhou, Yuxi Long, Mengchu Liu, Yongyu Li, Zhen Yi, Panfeng Wang, and Qingjiong Zhang

State Key Laboratory of Ophthalmology, Zhongshan Ophthalmic Center, Sun Yat-sen University, Guangdong Provincial Key Laboratory of Ophthalmology and Visual Science, Guangzhou, China

Correspondence: Qingjiong Zhang, Pediatric and Genetic Eye Clinic, Zhongshan Ophthalmic Center, Sun Yat-sen University, 54 Xianlie Road, Guangzhou 510060, China; [zhangqji@mail.sysu.edu.cn](mailto:zhangqji@mail.sysu.edu.cn)

Panfeng Wang, Gene Diagnostic Lab, Genetic Eye Clinic, Zhongshan Ophthalmic Center, Sun Yat-sen University, 54 Xianlie Road, Guangzhou 510060, China; [wpf5113@163.com](mailto:wpf5113@163.com)

Yingwei Wang and Wenmin Sun contributed equally to this work and should therefore be regarded as equivalent authors.

**Received:** November 16, 2021

**Accepted:** April 28, 2022

**Published:** May 24, 2022

Citation: Wang Y, Sun W, Zhou J, et al. Different phenotypes represent advancing stages of *ABCA4*-associated retinopathy: A longitudinal study of 212 Chinese families from a tertiary center. *Invest Ophthalmol Vis Sci.* 2022;63(5):28. <https://doi.org/10.1167/iovs.63.5.28>

**PURPOSE.** To evaluate the nature and association of different phenotypes associated with *ABCA4* mutations in Chinese.

**METHODS.** All patients were recruited from our pediatric and genetic eye clinic. Detailed ocular phenotypes were characterized. The disease course was evaluated by long-term follow-up observation, with a focus on fundus changes. Cox regression was used to identify the factors associated with disease progression.

**RESULTS.** A systematic review of genetic and clinical data for 228 patients and follow-up data for 42 patients indicated specific features in patients with two *ABCA4* variants. Of 185 patients with available fundus images, 107 (57.8%) showed focal lesions restricted to the central macula without flecks. Among these 107 patients, 30 patients (28.0%) initially presented with relatively preserved visual acuity and inconspicuous performance on routine fundus screening. A pigmentary change in the posterior pole was observed in 22 of 185 patients (11.9%), and this change mimicked retinitis pigmentosa in 10 cases (45.5%). Follow-up visits and sibling comparisons demonstrated disease progression from cone-rod dystrophy, Stargardt disease, to retinitis pigmentosa. An earlier age of onset was associated with a more rapid decrease in visual acuity ( $P = 0.03$ ). Patients with two truncation variants had an earlier age of onset.

**CONCLUSION.** Phenotypic variation in *ABCA4*-associated retinopathy may represent sequential changes in a single disease: early-stage Stargardt disease may resemble cone-rod dystrophy, whereas the presence of diffuse pigmentation in the late stage may mimic retinitis pigmentosa. Recognizing the natural progression of fundus changes, especially those visualized by wide-field fundus autofluorescence, is valuable for diagnostics and therapeutic decision-making.

**Keywords:** *ABCA4*-associated retinopathy, longitudinal study, progression, genotype-phenotype

The ATP binding cassette subfamily A member 4 (*ABCA4*; HGNC: 34; OMIM: 601691) gene is located at *1p22.1* and encodes retina-specific ATP-binding cassette transporters.<sup>1-3</sup> To date, more than 1000 *ABCA4* variants have been reported.<sup>4</sup> Variants in *ABCA4* are the most common genetic cause of Stargardt disease (STGD1, MIM: 248200),<sup>1</sup> as well as inherited retinal diseases.<sup>5</sup> In addition to Stargardt disease, variants in *ABCA4* have been reported to contribute to cone-rod dystrophy (CORD3, MIM:604116)<sup>6</sup> and retinitis pigmentosa (RP19, MIM:601718).<sup>7,8</sup> It is unclear why mutations in *ABCA4* contribute to different disease entities. Multiple studies have demonstrated that mutations in the same genes can cause different retinal diseases; additionally, mutations in a single gene can show phenotypes that mimic other diseases at different stages, such as *RPGR*, *RPE65*, and *PRPH2*.<sup>9-11</sup> It is of value to characterize the spectrum of phenotypes

caused by *ABCA4* variants and the associations among them.

Although Stargardt disease is one of the most frequent inherited retinal diseases in Caucasians,<sup>5,12</sup> it is significantly less common in Chinese individuals.<sup>13</sup> Whole or targeted exome sequencing data from our laboratory revealed that *ABCA4*-associated retinopathy is very common in Chinese individuals, whereas only a small portion of the population has typical Stargardt disease phenotypes. The majority of patients had phenotypes ranging from CORD to RP. In this study, data for 228 patients from 212 families with two *ABCA4* variants were collected at our clinic and analyzed to further understand the nature of multiple *ABCA4* variant-related phenotypes and associations among these variable phenotypes. Further follow-up observation was performed on 42 patients, with a comparative analysis of 10 siblings.

To the best of our knowledge, this is the first comprehensive characterization of multiple phenotypes of *ABCA4*-associated retinopathy based on a systemic analysis of a large Chinese cohort, including a multistep bioinformatic analysis of variants in *ABCA4*, phenotypic analyses, review of follow-up data, and exploration of genotype-phenotype correlation in a statistical framework. These findings provide valuable insight into the natural progression of this common disease to aid in the development of diagnostic and therapeutic approaches.

## METHODS

### Subjects and Variants Identification

Genetic and clinical data for all patients with two *ABCA4* variants were collected from our Pediatric and Genetic Clinic and its associated Gene Diagnostic Lab at the Zhongshan Ophthalmic Centre, Guangzhou, China. The study adhered to the tenets of the Declaration of Helsinki, and written informed consent was obtained from the probands or their guardians before the collection of peripheral venous blood samples and clinical data. Genomic DNA was extracted from leukocytes.<sup>14</sup> This study was approved by the institutional review board of the Zhongshan Ophthalmic Centre.

### *ABCA4* Variant Identification and Confirmation

In our clinic and associated laboratory, exome sequencing data were available for at least 7092 unrelated individuals with different eye conditions, including 1019 with retinitis pigmentosa, 1217 with glaucoma, 1299 with high myopia, 492 healthy controls, and 3065 with other ocular conditions. Mutations in *ABCA4* were identified from our exome sequencing data. Whole-exome sequencing and targeted exome sequencing were performed as described previously.<sup>13,15</sup> The variants were initially filtered by multistep bioinformatics analyses as previously described.<sup>15</sup> Variants whose minor allele frequencies exceeded 0.01 in the general population gnomAD dataset (<http://gnomad.broadinstitute.org/>) were excluded.

The pathogenicity of all *ABCA4* missense variants were predicted by five in silico tools, including SIFT ([http://sift.jcvi.org/www/SIFT\\_enstsubmit.html](http://sift.jcvi.org/www/SIFT_enstsubmit.html)),<sup>16</sup> PolyPhen-2 (<http://genetics.bwh.harvard.edu/pph2/index.shtml>),<sup>17</sup> PROVEAN ([https://provean.jcvi.org/genome\\_submit\\_2/](https://provean.jcvi.org/genome_submit_2/)), REVEL (<https://sites.google.com/site/revel/genomics/>),<sup>18</sup> and CADD (<https://cadd.gs.washington.edu/>).<sup>19</sup> The prediction results obtained using REVEL and CADD were evaluated and compared with the 75% and 95% cutoff scores from the gnomAD data. BDGP (<http://www.fruitfly.org/> [in the public domain]) was used to predict the potential pathogenicity of splicing variants. The HGMD (<http://www.hgmd.cf.ac.uk/ac/index.php>) and ACMG/AMP<sup>20</sup> criteria were used to assess all potential pathogenic variants. Furthermore, *ABCA4* variants were confirmed by Sanger sequencing.<sup>21</sup> Co-segregation and genotype-phenotype analyses were subsequently conducted for available families.

### Review and Summary of Clinical Information

Clinical data for in-house patients who carried two pathogenic or likely pathogenic *ABCA4* variants and presented with *ABCA4*-associated retinopathy phenotypes were collected and further analyzed. Clinical information

was recorded, including the age of onset (AO), initial diagnosis, first symptoms, and ophthalmic examinations. The disease duration was calculated as the difference between the age of presentation and the AO. Ophthalmologic examinations were systemically conducted, including best-corrected visual acuity (BCVA), color fundus photography (CFP), scanning laser ophthalmoscopy (SLO), fundus autofluorescence (FAF), optical coherence tomography (OCT), and electroretinography (ERG). BCVA was measured using a Snellen-equivalent visual acuity test chart and transformed to the logarithm of the minimum angle of resolution (LogMAR) for statistical analyses. The ERG results were used to classify the patients into three subtypes as follows by referring to a previous classification system: Group A had normal scotopic and photopic responses, Group B showed a reduced photopic response with normal scotopic responses, and Group C showed reduced scotopic and photopic responses.<sup>22</sup> To characterize the progression and genotype-phenotype correlation in *ABCA4* variants, all patients were subgrouped collectively by genotype: M+M group (patients with two missense mutations), T+M group (patients with one missense and one truncation mutation), and T+T group (patients with two truncation mutations).<sup>23</sup> Nonsense, canonical splice-site changes, as well as frameshift alterations, were considered as truncation variants. A sibling with the same two variants in *ABCA4* but different disease duration was analyzed as an observation of progression unit.

### Statistical Analysis

Kaplan-Meier survival curves were used to evaluate visual acuity outcomes in the three genotype groups. The outcome was defined as the probability of having a BCVA over 1.0 (LogMAR). Furthermore, a Cox regression model was applied to reveal differences in the decreasing tendency of visual acuity among different genotype groups. The differences in AO among the three genotype groups were evaluated by Mann-Whitney *U* tests.

Kaplan-Meier survival estimates and Cox regression model analyses were performed using Stata (Version 16.0). Mann-Whitney *U* tests were performed using Statistics 25.0.

## RESULTS

### Variant Identification in *ABCA4*

In total, 228 patients from 212 Chinese families had two variants in *ABCA4*, including 44 families whose genetic information was previously reported by us.<sup>13,24–26</sup> Variants in all individuals were confirmed by Sanger sequencing, and 54 patients from 44 families were further confirmed to have biallelic mutations in *ABCA4* by co-segregation analyses (Supplementary Fig. S1). Among these families, a total of 217 variants (122 missense, 37 nonsense, 28 frameshift, 26 splice-site, and four in-frame deletion) in *ABCA4* was detected by exome sequencing, including 104 novel variants and 113 previously reported variants (Supplementary Table S1). Among the 122 missense variants, 121 (99.2%) were predicted to be pathogenic or likely pathogenic. These 217 variants were distributed across 47 of the 50 exons of *ABCA4*, except for exon 5, exon 26, and exon 50. The most common variant in *ABCA4* among our patients was c.1804C>T/p.Arg602Trp, which accounted for 3.4% (15/446) of the mutant alleles (Supplementary Fig. S2). The

c.5882G>A/p.Gly1961Glu variant was present in only one family in our cohort, despite previous reports indicating that it is the most common allele (971/7639, 12.7%) (Supplementary Fig. S3).

### Clinical Characterization

This was a tertiary center study in which all patients originated from China, predominately southern China. The 228 patients from 212 families with two *ABCA4* variants were subdivided into three groups: M+M (71 patients from 70 families), T+M (115 individuals from 105 families), T+T (42 patients from 37 families). All 228 patients presented with bilateral central vision defect and characteristic macular atrophy with or without yellowish flecks at the posterior pole, although only 62.7% (143/228) of patients were initially diagnosed with Stargardt disease or macular degeneration. Among the remaining 85 patients, 57.6% (49/85) were considered to have refractive error and amblyopia at the initial visit, and 42.4% (36/85) were initially diagnosed with CORN or RP. The AO among the 210 patients with available data ranged from two to 60 years (median 9.0; IQR 7.0–13.0), and 65.7% (138/210) experienced vision impairment before 10 years of age, 25.2% (53/210) experienced vision impairment in the second decade, and 9.0% (19/210) experienced vision impairment after 20 years of age. The BCVA at the first visit ranged from 0.05 to hand motion (LogMAR) (median 0.82; IQR 0.70–1.00). Among 209 available BCVA records at the first visit, 18.2% (38/209) had visual acuity worse than 1.30, 69.4% (145/209) between 1.30 and 0.52, and only 12.4% (26/209) had visual acuity better than 0.52. Values of 1.30 and 0.52 were the diagnostic criteria for blindness and low vision, respectively.

Fundus photographs at the first visit were available for 185 in-house patients, and the fundus was classified into four stages: Stage I, focal lesions restricted to the central macula, ranging from irregular pigmentary changes to a bull's-eye-like change or a specific "beaten-bronze" appearance; Stage II, typical macular lesion with characteristic yellowish flecks extending from the central fovea to beyond the vascular arcades; Stage III, obvious macular choriocapillaris atrophy with diffusely resorbed flecks; and Stage IV, extensive choriocapillaris atrophy with pigment deposited at the central posterior area or beyond. Among the 185 patients with fundus images, 57.8% (107/185) were classified as Stage I. Among them, 28.0% (30/107) had preserved visual acuity (BCVA  $\leq$  0.52 LogMAR). In addition, inconspicuous macular dystrophy on CFP, specific bull's-eye changes on FAF, and increased reflectivity of the external limiting membrane or macular atrophy on OCT scans could be observed during the extremely early stages of the disease. As the disease progressed, the hyper-autofluorescence ring became larger and the macula became thinner on OCT (Fig. 1). Stage II was found in 22.2% of patients (41/185), and Stage III was observed in 8.1% of patients (15/185) (Fig. 2). Pigment deposits of varying shapes, including nummular pigmentation and bone-spicule pigment deposits located at the posterior pole (Stage IV), were observed in 11.9% of patients (22/185). Among the 22 patients with Stage IV disease, 72.7% (16/22) suffered from vision impairment for more than 10 years, and 45.5% (10/22) were initially diagnosed with RP. The BCVA of 177 patients decreased slowly with age and advanced changes of the fundi (Supplementary Fig. S4). Wide-field fundus examination was available in 42 patients,

including 19 patients with Stage I, nine individuals with Stage II, six with Stage III, and eight with Stage IV. Patients with Stage I showed a relatively preserved peripheral area with normal autofluorescence. Among patients with Stage II or III, a wide scope of flecks in the mid-periphery was clearly observed. The flecks expanded and increased, and those close to the macular vascular dome might be resorbed, with a change from hyper-autofluorescence to hypo-autofluorescence during disease progression. Flecks in varying conditions were more evident on wide-field FAF images than on CFP. Atrophic retinal pigment epithelium (RPE) lesions with variable shapes in the mid-periphery and pigment deposits extending from the central area to the mid-peripheral retina could be observed in SLO images for patients with Stage IV (Fig. 3).

OCT examinations were conducted on 157 individuals, all of whom presented with atrophic changes in central macula, including thickening of the external limiting membrane, structural irregularation of the outer retinal layer, and loss of the ellipsoid zone. ERG results were available for 88 patients, including 19.3% (17/88) in Group A, 22.7% (20/88) in Group B, and 58.0% (51/88) in Group C (Supplementary Figs. S5–7). All clinical characteristics of *ABCA4*-associated Stargardt disease in Chinese patients are outlined in Supplementary Table S2.

### Progression of *ABCA4*-Associated Retinopathy

The fundus changes in 42 in-house patients with long-term follow-up data and 10 siblings with the same mutations were summarized in detail. The follow-up duration was one to 20 years. Sequential fundus progression was observed in 61.5% of subjects (32/52), including 26 patients and six siblings. Among the 32 patients, 25 patients initially presented with Stage I and showed advanced fundus changes over time, including 13 patients who advanced to Stage II, 6 patients with progression to Stage III, and 6 patients with progression to Stage IV. Among three patients initially classified as Stage II, one advanced to Stage III and two advanced to Stage IV. The remaining four patients with initial Stage III fundus change progressed to Stage IV. The other twenty patients showed no fundus progression during follow-up (15 in Stage I, three in Stage II, and two in Stage IV) (Fig. 4, Supplementary Fig. S8). The nature of disease progression, especially changes in the fundus, was further supported by an analysis of the fundus of all 172 in-house patients considering the disease duration. Almost 84.6% of patients (88/104) with a disease duration less than two years presented with Stage I. Stage II and Stage III were dominant (63.4%, 26/41) among patients with a disease duration of two to 10 years. Of the patients with a disease duration over 10 years, 59.3% (16/27) were in Stage IV (Fig. 5).

Based on the BCVA and AO data for patients during follow-up, Kaplan-Meier curves were generated to predict tendency of vision deterioration among patients in the three genotype subgroups, identified by BCVA > 1.0 (LogMAR). Based on BCVA outcomes, vision deterioration occurred earlier in the T+T subgroup than in the T+M subgroup. BCVA for periods of over 10 years could not be evaluated for patients in the M+M group owing to insufficient follow-up data (Supplementary Fig. S9A). However, there was no significant difference among different genotype groups by a univariate Cox regression model. In a multivariate model including both genotype and AO, patients with an earlier AO presented with a higher risk for BCVA > 1.0 (LogMAR)



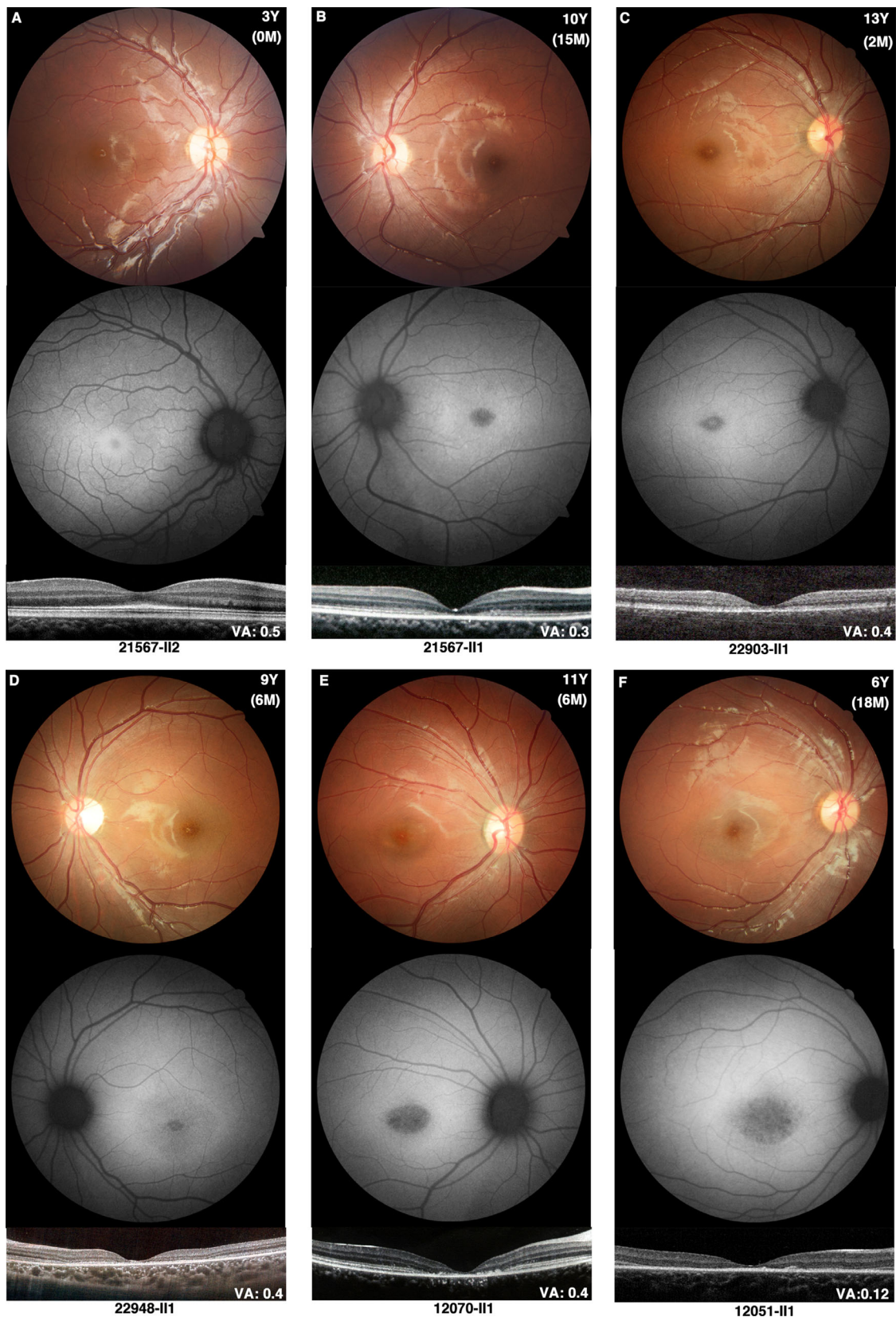


**FIGURE 1.** Fundus photography, FAF images and OCT results showing the early stage of *ABCA4*-associated retinopathy (Stage D). (A) Patient 21567-II2 was the sister of patient 21567-III1 (B) and did not show reduced central vision. Color fundus photography showed inconspicuous changes and relatively preserved visual acuity. Small-scale bull's-eye-like macular degeneration was observed on FAF imaging, and increased hyperreflectivity in the external limiting membrane and outer nuclear layer was found on OCT examination. (B–F) Various degrees of irregular pigment mottling were observed on fundus photography, decreased autofluorescence in the macular region surrounded by an increased autofluorescence parafoveal ring was found on FAF imaging, and macular atrophy was seen on OCT scans. The increased autofluorescence parafoveal ring became larger as the disease duration increased. The disease duration is shown in parentheses.

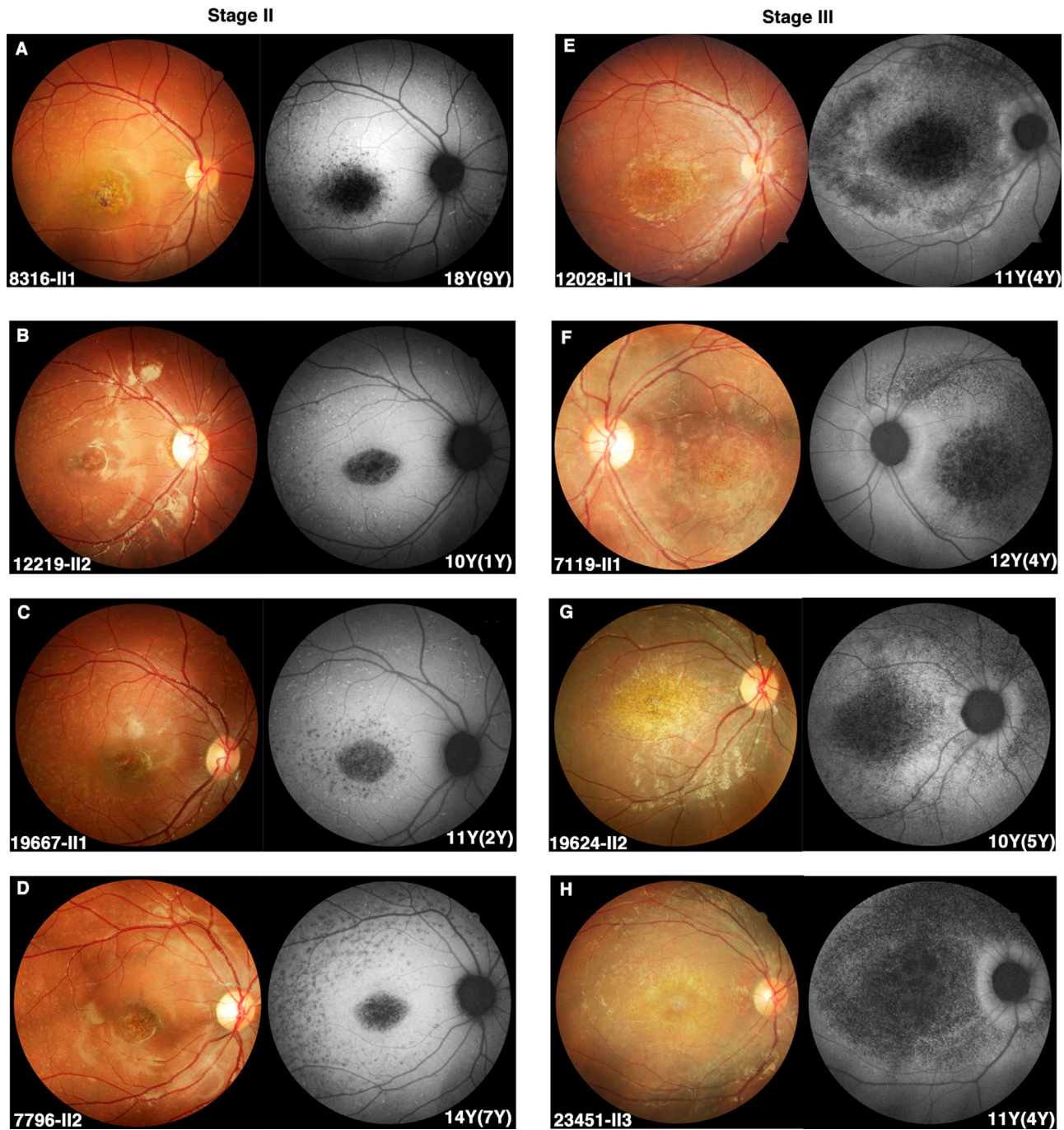


**FIGURE 2.** Fundus photography and FAF images showing the typical (Stage II) and atypical (Stage III) fundus presentation of *ABCA4*-associated retinopathy. (A–D) Specific yellowish flecks extending from central to vascular arcades, macular dystrophy on fundus photography, and corresponding hyper-autofluorescence or hypo-autofluorescence flecks on FAF (Stage II). (E–H) Flecks were partly resorbed, and choroid atrophy was detected in the macula region on color fundus photography. A heterogenous background with an enlarged area of hypo-autofluorescence was observed on the FAF image (Stage III). The disease duration is shown in parentheses.

(HR [95% confidence interval]: 0.87 [0.77-0.99],  $P = 0.032$ ). A scatter plot showed a decreasing tendency, indicating a correlation between the AO and the BCVA (LogMAR/years) (Supplementary Fig. S9B). In addition, all patients in the T+T group had an earlier AO than that of patients with two missense variants ( $P = 0.003$ ). Patients in the T+M group also showed a significantly earlier AO than that of patients in the M+M group ( $P = 0.026$ ) (Supplementary Fig. S9C).

## DISCUSSION

*ABCA4* is the most frequently implicated gene for inherited retinal degeneration based on a comprehensive review of our previous studies and a large cohort of 3197 families in the United Kingdom.<sup>5</sup> To our knowledge, this cohort of 228 patients from 212 families with two *ABCA4* mutations represents the largest cohort of Chinese patients



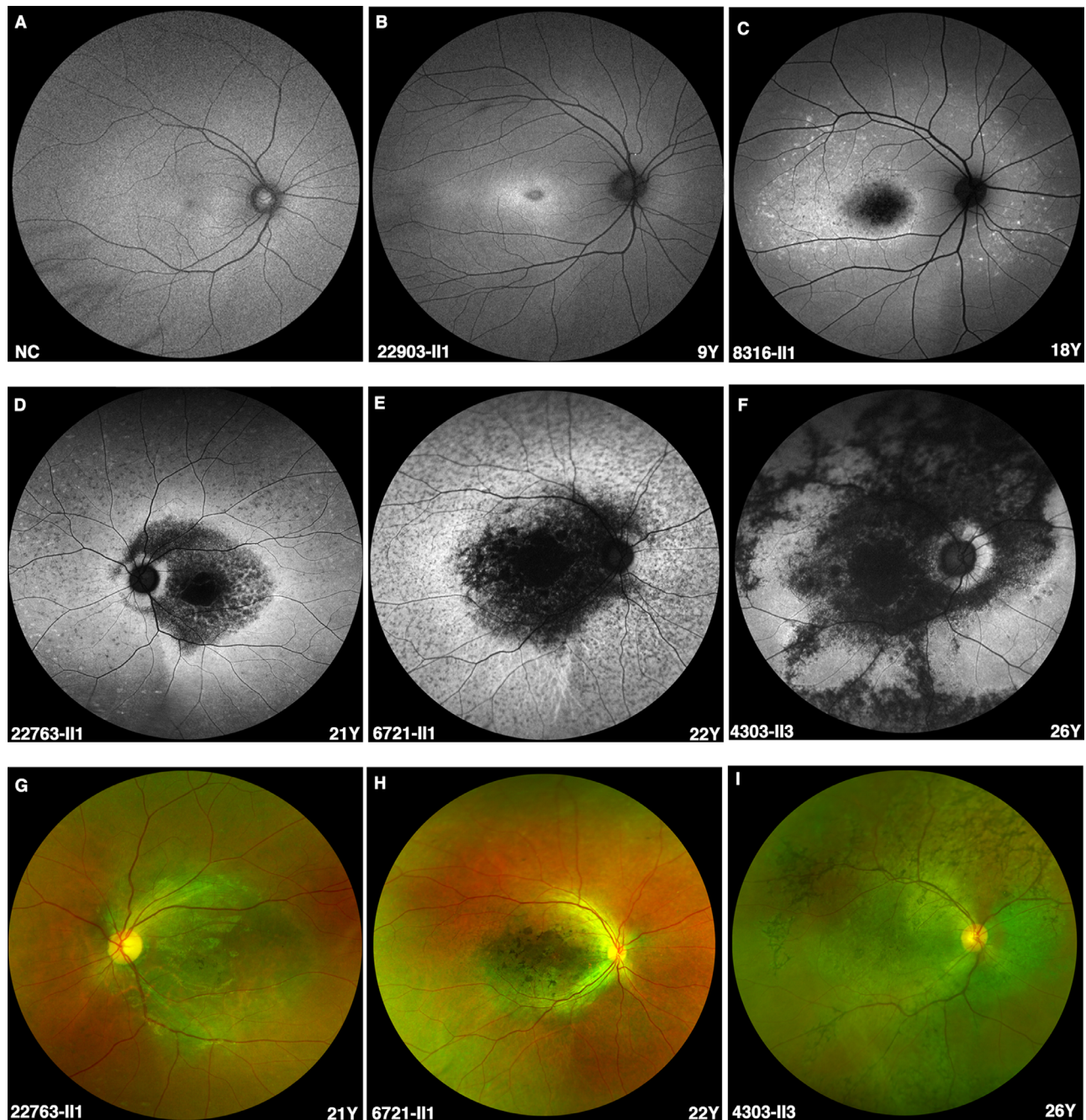


**FIGURE 3.** Wide-field fundus images of different fundus stages among patients with *ABCA4*-associated retinopathy. (A) Normal control. (B) Typical bull's-eye macular degeneration on FAF image (Stage I). (C) Hypo-autofluorescence change at the macular region with hyper-autofluorescence flecks scatter at the vascular arcades (Stage II). (D, G) Expanded retinal degeneration area observed at the posterior pole, showing an enlarged hypo-autofluorescence area on the FAF image. Hyper-autofluorescence and hypo-autofluorescence flecks could be found at the periphery (Stage III). (E, H) Pigmentary foci on the macular area and many hypo-autofluorescence flecks could be found at the periphery on FAF images (Stage IV). (F, I) Pigment deposits were extended from the macular area to the periphery in the advanced stage (Stage IV).

with *ABCA4*-associated retinopathy. Multiple and atypical phenotypes may hinder the recognition of this retinopathy in Chinese patients. A clear, sequential pattern associated with different phenotypes of *ABCA4*-associated retinopathy was established from genotype-based systemic analyses of clinical data for 228 patients from 212 Chinese families, including data from the long-term follow-up of 42 patients and data comparisons from ten siblings. These data

demonstrated that the phenotypic heterogeneity of *ABCA4*-associated retinopathy might reflect the sequential progression of a single disease, in which the early stage of the disease resembles cone-rod dystrophy without flecks (Stage I), followed by Stargardt disease with yellow flecks (Stage II), progression to enlarged diffuse macular degeneration with flecks resorbing (Stage III), and finally pigmentation from the central macular to mid-peripheral retinal area, mimicking

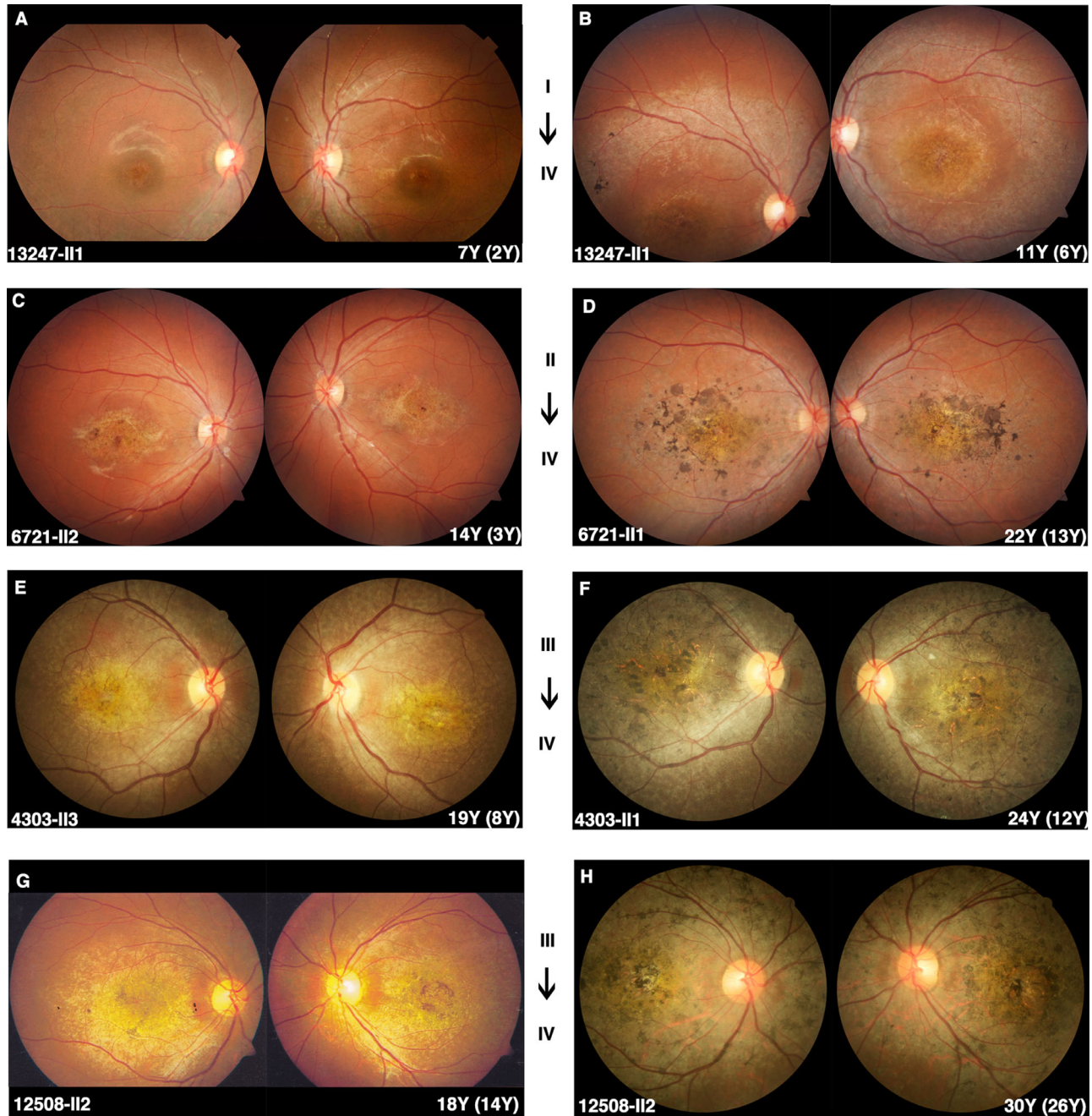


**FIGURE 4.** Fundus changes in the progression of *ABCA4*-associated retinopathy in our study. (A, B) Confined macular degeneration (Stage I) was observed in patient 13247-II1 at the first visit. A specific “beaten-bronze” macular appearance with a few bone spicule pigments scattered at the vascular dome (Stage IV) was found during the follow-up examination. (C, D) One sibling with the same biallelic *ABCA4* variants, confirmed by co-segregation. The younger patient 6721-II2 showed specific macular dystrophy with inconspicuous flecks (Stage II) and her sister 6721-II-1 had nummular or bone spicule pigments deposited at the macular area (Stage IV). (E, F) Another follow-up sibling with the same *ABCA4* variants. The younger patient 4303-II3 showed a specific “beaten-bronze” macular appearance plus choroid atrophy (Stage III), whereas his brother 4303-II1 had pigmentary changes at the posterior pole (Stage IV). (G, H) The long-term follow-up data for patient 2508-II1 showed typical enlarged macular degeneration (Stage III) that progressed to the advanced stage (Stage IV). The disease duration is shown in parentheses.

retinitis pigmentosa (Stage IV). These serially progressive fundus changes were observed among our in-house patients with follow-up and siblings. Analyzing the predominance of these four fundus stages in patients with different disease durations among all in-house patients further supported the natural progression of *ABCA4*-associated retinopathy. *ABCA4*-associated retinopathy involves a progressive degen-

eration from macula-only disease to widespread retinal dystrophy due to photoreceptor loss.<sup>27–29</sup> However, longitudinal prospective studies of the progression of *ABCA4*-associated retinopathy based on a large cohort are lacking. Disease progression can be characterized in detail by wide-field fundus autofluorescence on SLO, providing a basis for assessing the efficacy of novel treatments for *ABCA4*-



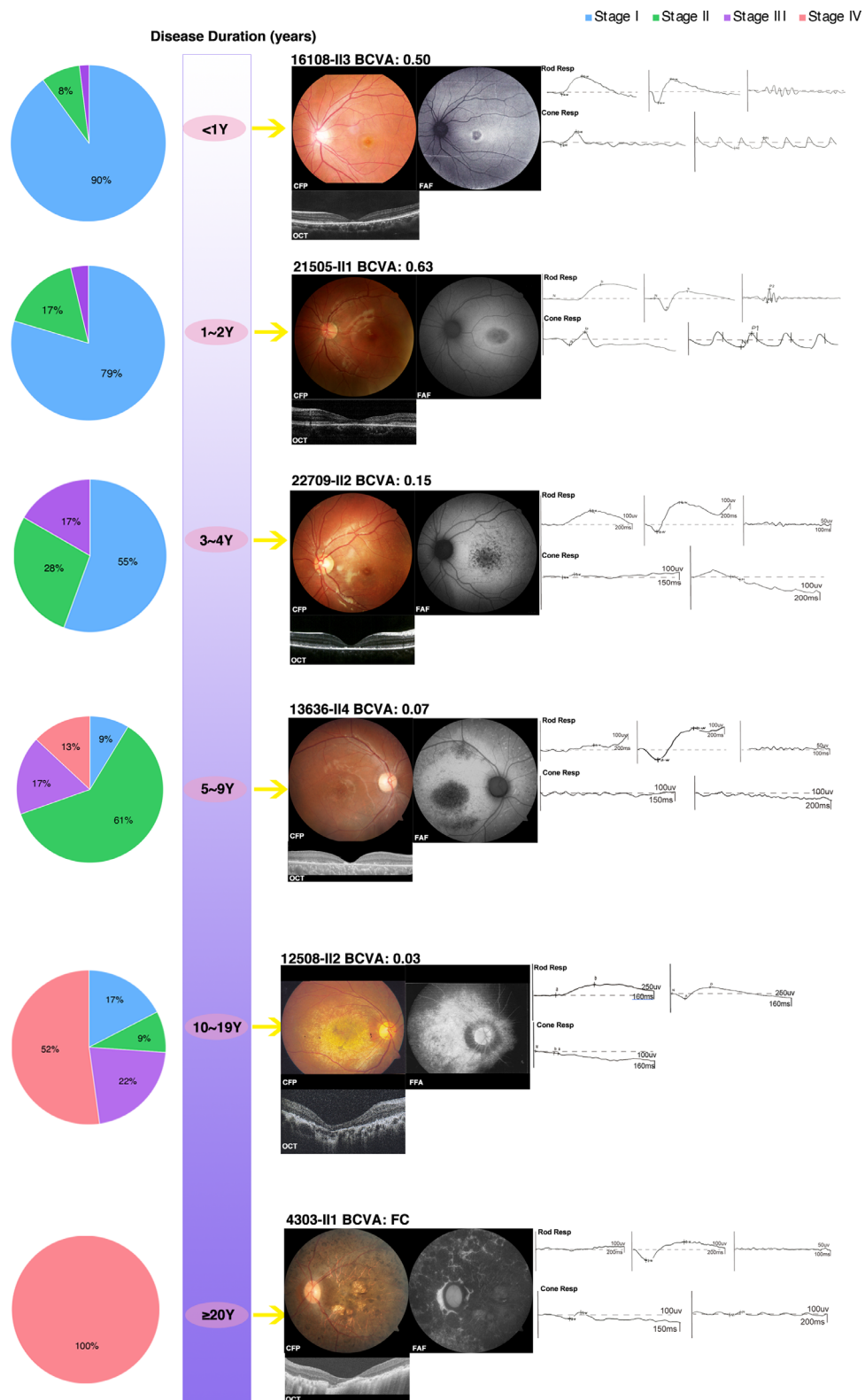


**FIGURE 5.** Schematic diagram of the progressive nature of *ABCA4*-associated retinopathy. The disease duration was calculated as the difference between the age of presentation and the age of onset. As the disease duration increased, the fundus changed from early typical bull's-eye macular degeneration (Stage I) to advanced pigmentary degeneration (Stage IV). The OCT examinations showed macular atrophy that developed into a serious choroid structure disorder. ERG showed normal rod and cone responses at the early stage, while cone and rod dystrophy occurred at the advanced stage. FFA, fluorescein fundus angiography.



associated retinopathy, such as gene therapy or stem-cell therapy.<sup>30</sup> Understanding the natural progression of *ABCA4*-associated retinopathy and correlations among multiple phenotypes may provide valuable diagnostic markers and a basis for future disease management.

Since *ABCA4* was first identified as the cause of Stargardt disease,<sup>1</sup> wide phenotypic variability of *ABCA4*-associated retinopathy has been described, including bull's-eye maculopathy,<sup>31</sup> macular atrophy,<sup>32</sup> fundus flavimaculatus,<sup>33</sup> foveal sparing phenotype,<sup>34</sup> cone-rod dystrophy,<sup>8</sup> and retinitis pigmentosa.<sup>35</sup> The protein encoded by *ABCA4* is predominantly located in the outer segment disk membranes of photoreceptors<sup>36</sup> and functions in the translocation of a major lipofuscin fluorophore substance (A2E).<sup>37</sup> Protein dysfunction leads to the accumulation of toxic lipofuscin compounds in the retinal pigment epithelium and photoreceptor failure.<sup>38</sup> In an animal model of *ABCA4*-associated retinopathy, the accumulation of A2E was strongly associated with light intensity.<sup>39–41</sup> In addition, it has been found that rod cell death is enriched in the parafoveal and perifoveal regions in the early stage of macular degeneration.<sup>42</sup> These findings might explain the progressive nature of *ABCA4* retinopathy from initial bull's-eye macular degeneration to retinitis pigmentosa-like phenotypes in the advanced stage extending to the mid-peripheral area. Additionally, an earlier onset is associated with severer phenotypes, such as mid-peripheral retinal degeneration and wide-field choriocapillaris dystrophy.<sup>43,44</sup> The fundus images of *ABCA4*-associated Stargardt disease have previously been classified into four classic stages.<sup>33,45</sup> In this study, the fundus classification was reconfigured to define pigmentary changes confined to the posterior retina as the final stage (Stage IV), which might better illuminate the progression of *ABCA4*-associated Stargardt disease in the clinic.

Based on a series of previous studies and individual gene-level pathogenicity analysis from our tertiary center, the number of families identified with variants in *ABCA4* ranked the first. Previous Chinese cohort studies have focused on the genotype-phenotype relationship and differences in the genetic background of patients with variants in *ABCA4*,<sup>46,47</sup> as observed in our study. Several reasons might explain the relatively rare of reports for large case series on *ABCA4*-associated retinopathy among Chinese. For example, the varied phenotypes related to *ABCA4* and the low proportion of characteristic fundus changes with yellowish flecks may be challenging diagnostic obstacles for inexperienced ophthalmologists. Alternatively, the low frequency of obvious yellowish flecks on routine ophthalmoscopy may hinder the recognition of Stargardt disease in the clinic. Furthermore, Chinese patients might exhibit ethnicity-specific phenotypes, given the difference in melanin levels between this population and Caucasians.<sup>48</sup> The emergence and resorption of diffuse flecks from the vascular arcade to the mid-periphery were more evident on wide-field FAF imaging than CFP. Therefore the value of wide-field FAF examinations to assess the efficacy of candidate therapies should be emphasized.

Various studies have revealed the relationship between the pathogenicity of variants and disease severity.<sup>46,49,50</sup> Large cohort follow-up studies of patients with Stargardt disease caused by two *ABCA4* variants are rare. A longitudinal study has reported that patients with two null mutations might exhibit severe disease at an earlier time point.<sup>49</sup> Patients with childhood-onset *ABCA4*-associated Stargardt disease are more likely to experience more severe visual

acuity loss, accompanied by marked dysfunction of the photoreceptors on ERG and progressive spreading of RPE atrophy.<sup>27,51–54</sup> In this study, we highlighted that the AO influenced the vision impairment rate. An earlier AO in patients with truncation variants was also observed in our study. Therefore, the pathogenicity of variants may directly determine the progression and outcome of *ABCA4*-associated retinopathy.

In summary, multiple *ABCA4*-associated retinopathy phenotypes may represent sequential changes in a single disease, with the early stage resembling cone-rod dystrophy and the late stage showing diffuse pigmentation mimicking retinitis pigmentosa. Therefore, wide-field fundus autofluorescence examination is suggested as the first choice in the clinic. Our findings clearly delineated the natural progression of *ABCA4*-associated retinopathy, especially fundus changes, which is essential in the era of widespread clinical genetic testing and in the upcoming age of potential new intervention.

### Acknowledgments

Supported by grants from National Natural Science Foundation of China (NO. 81970837) and the Fundamental Research Funds of the State Key Laboratory of Ophthalmology.

Disclosure: **Y. Wang**, None; **W. Sun**, None; **J. Zhou**, None; **X. Li**, None; **Y. Jiang**, None; **S. Li**, None; **X. Jia**, None; **X. Xiao**, None; **J. Ouyang**, None; **Y. Wang**, None; **L. Zhou**, None; **Y. Long**, None; **M. Liu**, None; **Y. Li**, None; **Z. Yi**, None; **P. Wang**, None; **Q. Zhang**, None

### References

- Allikmets R. A photoreceptor cell-specific ATP-binding transporter gene (ABCR) is mutated in recessive Stargardt macular dystrophy. *Nat Genet.* 1997;17:122.
- Zernant J, Xie YA, Ayuso C, et al. Analysis of the *ABCA4* genomic locus in Stargardt disease. *Hum Mol Genet.* 2014;23:6797–6806.
- Nasonkin I, Illing M, Koehler MR, Schmid M, Molday RS, Weber BH. Mapping of the rod photoreceptor ABC transporter (ABCR) to 1p21-p22.1 and identification of novel mutations in Stargardt's disease. *Hum Genet.* 1998;102:21–26.
- Cornelis SS, Bax NM, Zernant J, et al. In silico functional meta-analysis of 5,962 *ABCA4* variants in 3,928 retinal dystrophy cases. *Hum Mutat.* 2017;38:400–408.
- Pontikos N, Arno G, Jurkute N, et al. Genetic basis of inherited retinal disease in a molecularly characterized cohort of more than 3000 families from the United Kingdom. *Ophthalmology.* 2020;127:1384–1394.
- Maugeri A, Klevering BJ, Rohrschneider K, et al. Mutations in the *ABCA4* (ABCR) gene are the major cause of autosomal recessive cone-rod dystrophy. *Am J Hum Genet.* 2000;67:960–966.
- Martínez-Mir A, Bayés M, Vilageliu L, et al. A new locus for autosomal recessive retinitis pigmentosa (RP19) maps to 1p13-1p21. *Genomics.* 1997;40:142–146.
- Cremers FP, van de Pol DJ, van Driel M, et al. Autosomal recessive retinitis pigmentosa and cone-rod dystrophy caused by splice site mutations in the Stargardt's disease gene ABCR. *Hum Mol Genet.* 1998;7:355–362.
- Nguyen XT, Talib M, van Schooneveld MJ, et al. RPGR-associated dystrophies: clinical, genetic, and histopathological features. *Int J Mol Sci.* 2020;21:835.

10. Li S, Xiao X, Yi Z, Sun W, Wang P, Zhang Q. RPE65 mutation frequency and phenotypic variation according to exome sequencing in a tertiary centre for genetic eye diseases in China. *Acta Ophthalmol.* 2020;98:e181–e190.
11. Boon CJ, den Hollander AI, Hoyng CB, Cremers FP, Klevering BJ, Keunen JE. The spectrum of retinal dystrophies caused by mutations in the peripherin/RDS gene. *Prog Retin Eye Res.* 2008;27:213–235.
12. Goetz KE, Reeves MJ, Gagadam S, et al. Genetic testing for inherited eye conditions in over 6,000 individuals through the eyeGENE network. *Am J Med Genet C Semin Med Genet.* 2020;184:828–837.
13. Wang P, Li S, Sun W, et al. An ophthalmic targeted exome sequencing panel as a powerful tool to identify causative mutations in patients suspected of hereditary eye diseases. *Transl Vis Sci Technol.* 2019;8:21.
14. Wang Q, Wang P, Li S, et al. Mitochondrial DNA haplogroup distribution in Chaoshanese with and without myopia. *Mol Vis.* 2010;16:303–309.
15. Li J, Jiang D, Xiao X, et al. Evaluation of 12 myopia-associated genes in Chinese patients with high myopia. *Invest Ophthalmol Vis Sci.* 2015;56:722–729.
16. Kumar P, Henikoff S, Ng PC. Predicting the effects of coding non-synonymous variants on protein function using the SIFT algorithm. *Nat Protoc.* 2009;4:1073–1081.
17. Adzhubei I, Jordan DM, Sunyaev SR. Predicting functional effect of human missense mutations using PolyPhen-2. *Curr Protoc Hum Genet.* 2013;Chapter 7:Unit7.20.
18. Ioannidis NM, Rothstein JH, Pejaver V, et al. REVEL: an ensemble method for predicting the pathogenicity of rare missense variants. *Am J Hum Genet.* 2016;99:877–885.
19. Rentzsch P, Witten D, Cooper GM, Shendure J, Kircher M. CADD: predicting the deleteriousness of variants throughout the human genome. *Nucleic Acids Res.* 2019;47:D886–D894.
20. Richards S, Aziz N, Bale S, et al. Standards and guidelines for the interpretation of sequence variants: a joint consensus recommendation of the American College of Medical Genetics and Genomics and the Association for Molecular Pathology. *Genet Med.* 2015;17:405–424.
21. Chen Y, Zhang Q, Shen T, et al. Comprehensive mutation analysis by whole-exome sequencing in 41 Chinese families with Leber congenital amaurosis. *Invest Ophthalmol Vis Sci.* 2013;54:4351–4357.
22. Lois N, Holder GE, Bunce C, Fitzke FW, Bird AC. Phenotypic subtypes of Stargardt macular dystrophy-fundus flavimaculatus. *Arch Ophthalmol.* 2001;119:359–369.
23. Del Pozo-Valero M, Riveiro-Alvarez R, Blanco-Kelly F, et al. Genotype-phenotype correlations in a Spanish cohort of 506 families with biallelic ABCA4 pathogenic variants. *Am J Ophthalmol.* 2020;219:195–204.
24. Huang L, Xiao X, Li S, et al. Molecular genetics of cone-rod dystrophy in Chinese patients: new data from 61 probands and mutation overview of 163 probands. *Exp Eye Res.* 2016;146:252–258.
25. Xin W, Xiao X, Li S, Jia X, Guo X, Zhang Q. Identification of genetic defects in 33 probands with Stargardt disease by WES-based bioinformatics gene panel analysis. *PLoS One.* 2015;10:e0132635.
26. Huang L, Zhang Q, Li S, et al. Exome sequencing of 47 Chinese families with cone-rod dystrophy: mutations in 25 known causative genes. *PLoS One.* 2013;8:e65546.
27. Cideciyan AV, Swider M, Aleman TS, et al. ABCA4 disease progression and a proposed strategy for gene therapy. *Hum Mol Genet.* 2009;18:931–941.
28. Cideciyan AV, Swider M, Schwartz SB, Stone EM, Jacobson SG. Predicting progression of ABCA4-associated retinal degenerations based on longitudinal measurements of the leading disease front. *Invest Ophthalmol Vis Sci.* 2015;56:5946–5955.
29. Fakin A, Robson AG, Fujinami K, et al. Phenotype and progression of retinal degeneration associated with nullizigosity of ABCA4. *Invest Ophthalmol Vis Sci.* 2016;57:4668–4678.
30. von Rückmann A, Fitzke FW, Bird AC. Distribution of fundus autofluorescence with a scanning laser ophthalmoscope. *Br J Ophthalmol.* 1995;79:407–412.
31. Michaelides M, Chen LL, Brantley MA, Jr., et al. ABCA4 mutations and discordant ABCA4 alleles in patients and siblings with bull's-eye maculopathy. *Br J Ophthalmol.* 2007;91:1650–1655.
32. Michaelides M, Hunt DM, Moore AT. The genetics of inherited macular dystrophies. *J Med Genet.* 2003;40:641–650.
33. Fishman GA. Fundus flavimaculatus. A clinical classification. *Arch Ophthalmol.* 1976;94:2061–2067.
34. Fujinami K, Sergouniotis PI, Davidson AE, et al. Clinical and molecular analysis of Stargardt disease with preserved foveal structure and function. *Am J Ophthalmol.* 2013;156:487–501.e481.
35. Martínez-Mir A, Paloma E, Allikmets R, et al. Retinitis pigmentosa caused by a homozygous mutation in the Stargardt disease gene ABCR. *Nat Genet.* 1998;18:11–12.
36. Illing M, Molday LL, Molday RS. The 220-kDa rim protein of retinal rod outer segments is a member of the ABC transporter superfamily. *J Biol Chem.* 1997;272:10303–10310.
37. Mata NL, Weng J, Travis GH. Biosynthesis of a major lipofuscin fluorophore in mice and humans with ABCR-mediated retinal and macular degeneration. *Proc Natl Acad Sci USA.* 2000;97:7154–7159.
38. Molday RS, Zhong M, Quazi F. The role of the photoreceptor ABC transporter ABCA4 in lipid transport and Stargardt macular degeneration. *Biochim Biophys Acta.* 2009;1791:573–583.
39. Mata NL, Tzekov RT, Liu X, Weng J, Birch DG, Travis GH. Delayed dark-adaptation and lipofuscin accumulation in ABCR+/- mice: implications for involvement of ABCR in age-related macular degeneration. *Invest Ophthalmol Vis Sci.* 2001;42:1685–1690.
40. Maeda A, Maeda T, Golczak M, Palczewski K. Retinopathy in mice induced by disrupted all-trans-retinal clearance. *J Biol Chem.* 2008;283:26684–26693.
41. Maeda A, Maeda T, Golczak M, et al. Involvement of all-trans-retinal in acute light-induced retinopathy of mice. *J Biol Chem.* 2009;284:15173–15183.
42. Okano K, Maeda A, Chen Y, et al. Retinal cone and rod photoreceptor cells exhibit differential susceptibility to light-induced damage. *J Neurochem.* 2012;121:146–156.
43. Holtan JP, Aukrust I, Jansson RW, et al. Clinical features and molecular genetics of patients with ABCA4-retinal dystrophies. *Acta Ophthalmol.* 2021;99:e733–e746.
44. Bertelsen M, Zernant J, Larsen M, Duno M, Allikmets R, Rosenberg T. Generalized choriocapillaris dystrophy, a distinct phenotype in the spectrum of ABCA4-associated retinopathies. *Invest Ophthalmol Vis Sci.* 2014;55:2766–2776.
45. Cremers FPM, Lee W, Collin RWJ, Allikmets R. Clinical spectrum, genetic complexity and therapeutic approaches for retinal disease caused by ABCA4 mutations. *Prog Retin Eye Res.* 2020;79:100861.
46. Sun Z, Yang L, Li H, et al. Clinical and genetic analysis of the ABCA4 gene associated retinal dystrophy in a large Chinese cohort. *Exp Eye Res.* 2021;202:108389.



47. Liu X, Meng X, Yang L, et al. Clinical and genetic characteristics of Stargardt disease in a large Western China cohort: Report 1. *Am J Med Genet C Semin Med Genet*. 2020;184:694–707.
48. Chan IL, Cohen S, da Cunha MG, Maluf LC. Characteristics and management of Asian skin. *Int J Dermatol*. 2019;58:131–143.
49. Di Iorio V, Orrico A, Esposito G, et al. Association between genotype and disease progression in Italian Stargardt patients: a retrospective natural history study. *Retina*. 2019;39:1399–1409.
50. Simonelli F, Testa F, Zernant J, et al. Genotype-phenotype correlation in Italian families with Stargardt disease. *Ophthalmic Res*. 2005;37:159–167.
51. Fujinami K, Lois N, Davidson AE, et al. A longitudinal study of Stargardt disease: clinical and electrophysiologic assessment, progression, and genotype correlations. *Am J Ophthalmol*. 2013;155:1075–1088.e1013.
52. Rotenstreich Y, Fishman GA, Anderson RJ. Visual acuity loss and clinical observations in a large series of patients with Stargardt disease. *Ophthalmology*. 2003;110:1151–1158.
53. McBain VA, Townend J, Lois N. Progression of retinal pigment epithelial atrophy in Stargardt disease. *Am J Ophthalmol*. 2012;154:146–154.
54. Fujinami K, Zernant J, Chana RK, et al. Clinical and molecular characteristics of childhood-onset Stargardt disease. *Ophthalmology*. 2015;122:326–334.